P2.22 Impact of surface roughness length on typhoon simulations

Akiyoshi Wada*[1] and Nadao Kohno[2]
[1]Meteorological Research Institute
[2]Japan Meteorological Agency

1. Introduction

Surface roughness lengths over the ocean are varied by ocean waves. The surface roughness length is usually calculated as a surface boundary process in an atmosphere model to determine air-sea exchange coefficients for momentum, sensible and latent heat fluxes and profiles of atmospheric ingredients based on similarity theory. The sensible and latent heat fluxes play a crucial role in the development of a tropical cyclone, while the momentum flux drives the upper ocean beneath a tropical cyclone, resulting in sea-surface cooling by passage of a tropical cyclone. The exchange coefficient for the momentum flux is also related to surface friction, which plays roles in the reduction of tangential winds and in the production of radial inflow. Kohno et al (2006) examined the impact of surface roughness length on simulations of ocean waves and Typhoon Tokage in 2004 by using an atmosphere-wave coupled model. However, the result was limited only in a single typhoon case and the effect of sea surface cooling was not included in the atmosphere-wave coupled model used in Kohno et al (2006) .

In order to understand the effect of surface roughness lengths on simulations of tropical cyclones, the impacts of surface roughness lengths on simulations of tropical cyclones are investigated for Typhoons Choi-wan (2009) and Fanapi (2010) by sensitivity experiments using a nonhydrostatic atmosphere model (NHM) coupled with the third generation ocean wave model and a multi-layer ocean model (Wada et al., 2010).

Table 1 List of surface roughness length scheme and its formulation.

Scheme and acronym	Formulation
Janssen(1991) [JA1]	$\frac{gz_0}{u_*^2} = 0.010\left(1-\frac{\tau_w}{\tau}\right)^{-\frac{1}{2}}$
Smith et al(1992) [SM1]	$\frac{gz_0}{u_*^2} = 0.48\left(\frac{u*}{c_p}\right)$
Taylor and Yelland (2001) [TY1]	$\frac{gz_0}{u_*^2} = 1200\left(\frac{H_w}{L_w}\right)$
Charnock (1955) [CH1]	$\frac{gz_0}{u_*^2} = \alpha = 0.0185$
Kondo (1975) [KO1]	$z_0 = \exp\left\{\ln z_{10} - \kappa\left[C_D(10m)^{-1/2}\right]\right\}$

This study addresses the impacts of surface roughness lengths on tracks and intensities of Choi-wan and Fanapi, those on the relation of surface wind speeds to surface roughness lengths and drag coefficients and those on their horizontal distributions in an atmosphere-wave-ocean coupled system. A list of schemes for calculating surface roughness length and acronyms used in this study is shown in Table 1.

2. Models and experimental design

Numerical simulations were performed for Choi-wan and Fanapi respectively by using the atmosphere-wave-ocean coupled model. The latter typhoon is one of targeted typhoons during the period of the Impact of Typhoons on the Ocean in the Pacific (ITOP) campaign observation. The coupled model covered a 3240 km x 3960 km computational domain with a horizontal grid spacing of 6 km for Choi-wan and a 2000 km x 1800 km with a horizontal grid spacing of 2 km for Fanapi. The coupled model had 40 vertical levels with variable intervals from 40 m for the near-surface layer to 1180 m for the uppermost layer. The coupled model had maximum height approaching nearly 23 km. The integration time was 96 hours with a time step of 15 seconds for Choi-wan and was 72 hours with a time step of 6 seconds for Fanapi. The time step of the ocean model was 90 seconds for Choi-wan and 36 seconds for Fanapi, and that of the ocean wave model was 10 minutes for both typhoons. Detail descriptions associated with physical schemes in the NHM were documented in Wada (2009). Wind speeds at 10-m height and drag coefficients were calculated respectively by the method proposed by Louis et al. (1982) after the surface roughness lengths were calculated by one of five formulations (Table 1).

Initial and boundary conditions in the atmosphere were obtained from global analysis data with a horizontal resolution of 20 km archived in the Japan Meteorological Agency. The time interval of the atmospheric lateral condition was six hours. Initial conditions in the ocean were obtained from the daily oceanic reanalysis datasets with horizontal resolutions of 0.1º calculated by the Meteorological Research Institute multivariate ocean variational estimation (MOVE) system (Usui, et al., 2006). The end figure '1' of acronyms in Table 1 indicates that this study used the oceanic reanalysis dataset with a horizontal resolution of 0.1 º.

*[1] Corresponding author address: Akiyoshi Wada. Meteorological Research Institute, 1-1 Nagamine Tsukuba Ibaraki 305-0052, Japan.
e-mail: awada@mri-jma.go.jp

3. Results

3.1. Track and Intensity

Figure 1 illustrates the results of track and central pressure simulations together with best track data for Choi-wan. Figure 1a indicates that the impact of an exchange of surface roughness length formulation on a track simulation is negligibly small. In contrast, a maximum difference of simulated central pressures between SM1 and KO1 exceeds 6 hPa at 1800 UTC on 18 September in 2009. The maximum difference is found during the mature phase of simulated Choi-wan (Fig. 1b). All simulated central pressures are lower than the best-track central pressure after 30-hour integration (30 h).

Figure 2 illustrates the results of track and central pressure simulations with best track data for Fanapi. All simulated tracks show a northward bias after 18 h (Fig.2a). This result reveals that the track simulation is independent of a choice of surface roughness length scheme. A maximum difference of simulated central pressures between CH1 and SM1 exceeds 8 hPa at 0000 UTC on 19 September in 2010. Unlike the results of the simulations of central pressures for Choi-wan, all simulated central pressures are higher than the best-track central pressure for Fanapi. Nevertheless, the two simulations suggest that simulated central-pressures depend on the formulation of surface roughness lengths (Figs 1b and 2b). The difference becomes large markedly when the simulated typhoon intensifies again after 36 h and simulated Fanapi continuously intensifies.

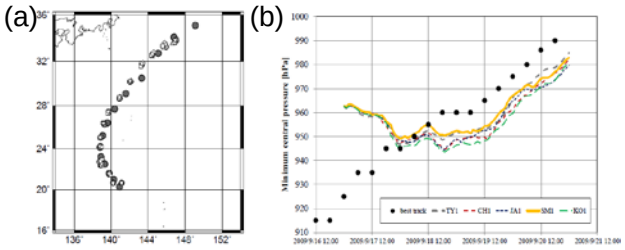

Figure 1 (a) Regional Specialized Meteorological Center-Tokyo best track (dark gray circles) and simulated tracks for Typhoon Choi-wan (2009) from 0000 UTC on 17 to 1200 UTC on 20 September in 2009, and (b) time series of best-track and simulated central pressures. Note that light small circles indicate the result in TY1, open diamonds CH1, light gray triangles JA1, open squares SM1 and open inverse triangles KO1.

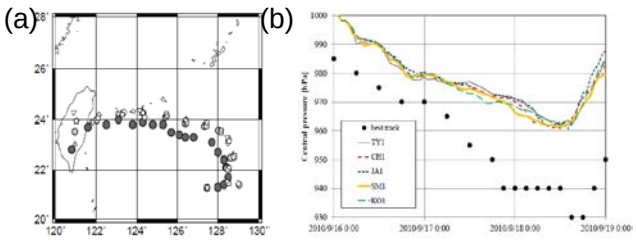

Figure 2 Same as Fig. 1 except for Typhoon Fanapi (2010) from 0000 UTC on 16 to 0000 UTC 19 September in 2010.

3.2. Surface roughness length and drag coefficient

The relation of 10-m wind speed to surface roughness length and drag coefficient calculated by the coupled model is investigated in each surface-roughness-length formulation for Choi-wan (Fig. 3a and 3c) and Fanapi (Fig. 4a and 4c). Figures 3a and 4a indicates that surface roughness lengths in SM1 and TY1 are remarkably higher than those in JA1, CH1 and KO1 in both typhoons.

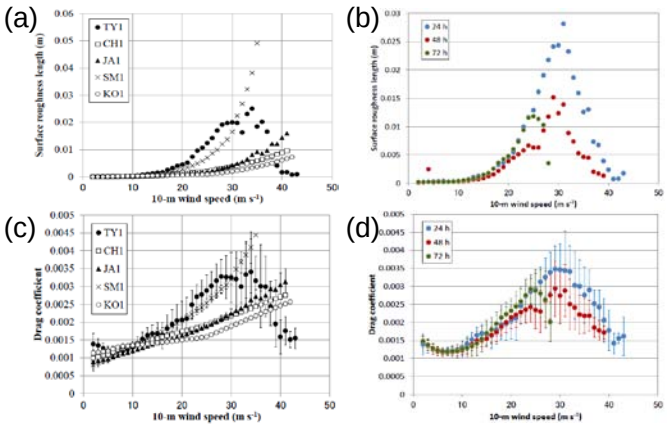

Figure 3 Relation of 10-m wind speed to surface roughness length (a) at 24 h and (b) at 24 h, 48h and 72 h in TY1 and that to drag coefficient (c) at 24 h and (d) at 24 h, 48h and 72 h in TY1 for Typhoon Choi-wan in 2009.

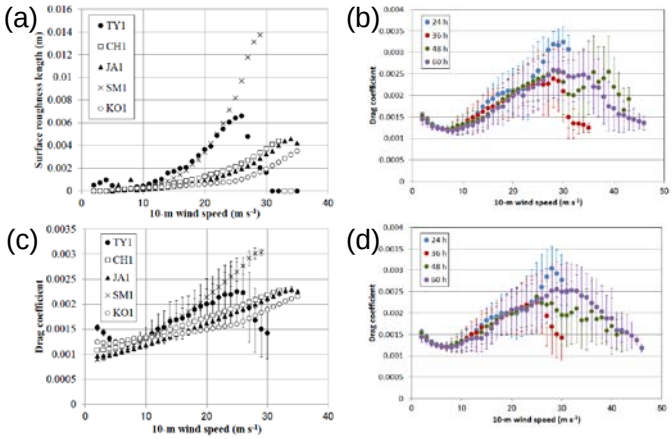

Figure 4 Relation of 10-m wind speed to surface roughness length (a) at 36 h and (b) at 24 h, 36 h, 48 h and 60 h in TY1 and that to drag coefficient (c) at 36 h and (d) at 24 h, 36 h, 48 h and 60 h in TY1 for Typhoon Fanapi in 2010.

Unlike the results in SM1, surface roughness lengths (Figs. 3b and 4b) and drag coefficients (Figs. 3d and 4d) in TY1 level off when 10-m wind speeds are relatively high. The value of wind speed at the peak of surface roughness length and drag coefficient differs between Choi-wan and Fanapi and it depends on the phase (integration time) of these typhoons. Both high values of surface roughness lengths and drag coefficients in SM1 and their monotonically increases may result in high central pressure (Fig. 1b), while low values of surface roughness lengths and drag coefficients under high surface winds in TY1 are related to low central pressures (Fig. 1b). A difference in central pressures between SM1 and TY1 clearly appears during the intensified phase in Choi-wan, probably because

a difference of surface roughness lengths and drag coefficients can directly affect the intensity simulations. However, central pressures in SM1 tend to be low in the case of Fanapi. This suggests that values of surface roughness lengths and drag coefficients are not simply related to values of simulated central pressures. It should be noted that drag coefficients in TY1 are high under relatively low winds (Figs. 3c-d and 4c-d), which is consistent with the observation reported by Edson et al. (2007).

3.3. Horizontal distributions

Figure 5 illustrates the horizontal distribution of wind speeds at 20-m height in SM1 (Figs. 5a and 5d), JA1 (Figs. 5b and 5e) and TY1 (Figs. 5c and 5f) at 24 h (Figs. 5a-c) and 72 h (Figs. 5d-f) for Choi-wan. The 20-m height is the lowermost level in the NHM. After rapid intensification, the distribution of horizontal winds in JA1 comes close to an annular pattern at 24 h (Fig. 5b), but indeed, the distribution has a wave-number 1 pattern, where wind speeds are high at the southeastern side within the inner core. The horizontal distributions of 20-m wind speed in SM1 (Fig. 5a) and TY1 (Fig. 5c) have an asymmetric pattern and the winds in the northwestern side are remarkably weak. The asymmetric wind distributions are related to relatively high central pressures in SM1 and TY1 compared to simulated central pressure in JA1.

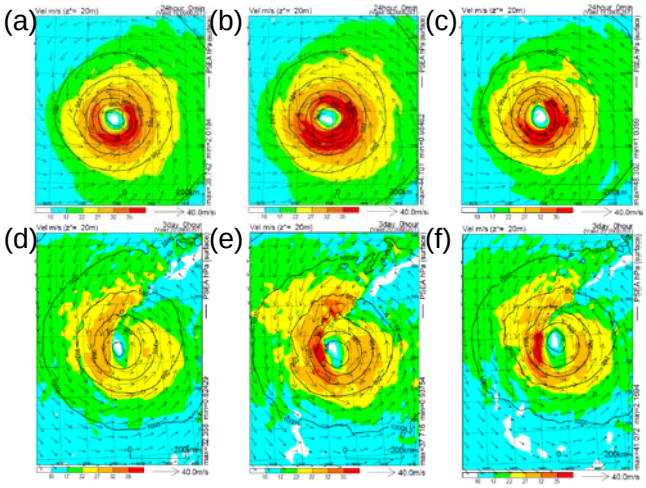

Figure 5 Horizontal distributions of 20-m wind speed (at the lowermost level) at 24 h for Choi-wan in (a) SM1, (b) JA1 and (c) TY1 and those at 60 h in (d) SM1, (e)JA1 and (f) TY1.

During the decaying phase of Choi-wan, wind speeds become high at the western side in JA1 and TY1 at 72 h (Figs. 5e and 5f). However, wind speeds in SM1 are relatively low at the area (Fig. 5d). The results suggest that a choice of surface-roughness-length scheme directly affect the horizontal distribution of wind speeds around the inner core from the developing to the decaying phase of Choi-wan.

Figure 6 illustrates the horizontal distribution of significant wave heights in SM1 (Figs. 6a and 6d), JA1 (Figs. 6b and 6e) and TY1 (Figs. 6c and 6f) at 24 h (Figs. 6a-c) and 72 h (Figs. 6d-f) for Choi-wan. At 24 h, significant wave heights have an axisymmetric patter where 20-m wind speeds are high (Figs. 5a-c). In addition, significant wave heights tend to be high on the right side along the track behind the typhoon. At 72 h, significant wave heights tend to be high on the right and left sides along the track behind the typhoon. The maximum value of significant wave height in TY1 is highest at 72 h although the value is the same at 24 h among the three experiments.

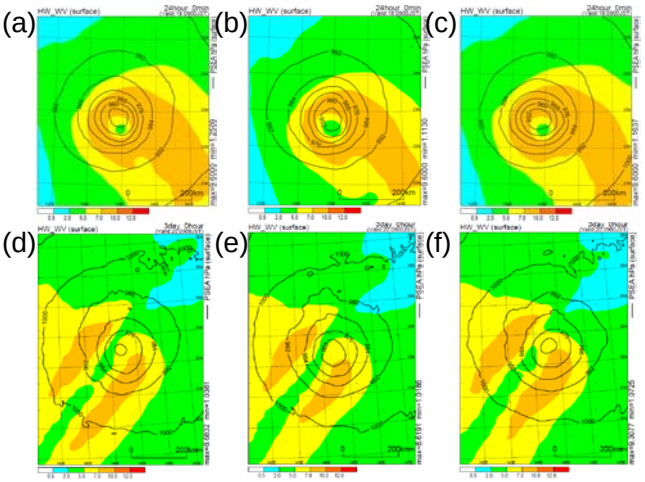

Figure 6 Horizontal distributions of significant wave height (at the lowermost level) at 24 h for Choi-wan in (a) SM1, (b) JA1 and (c) TY1.

Figure 7 illustrates the horizontal distribution of wind speeds at 20-m height in SM1 (Figs. 7a and 7d), JA1 (Figs. 7b and 7e) and TY1 (Figs. 7c and 7f) at 24 h (Figs. 7a-c) and 60 h (Figs. 7d-f) for Fanapi. During the intensification (at 24 h), wind speeds are high at the northeastern side in all cases and the distribution has markedly a wave-number 1 pattern. Wind speeds are highest in JA1 (Fig. 7b) and lowest in SM1 (Fig. 7a) among the three experiments However, there is no significant difference in central pressures among five experiments (Fig. 2b).

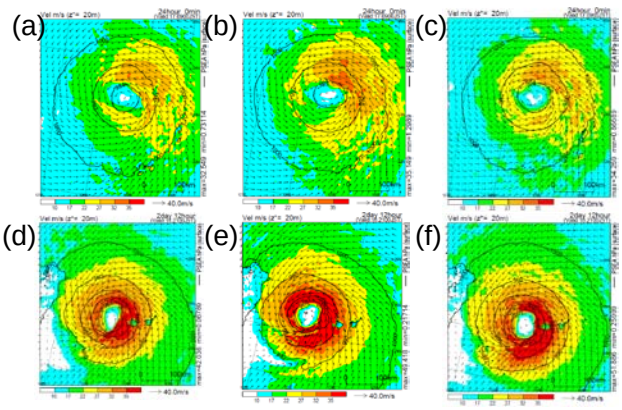

Figure 7 Same as Figure 5 except for Fanapi.

When a simulated central pressure reaches the minimum at 60 h, the horizontal distribution of wind speeds in JA1 comes close to an annular pattern (Fig. 7e). In contrast, the distributions in SM1 (Fig. 7d) and TY1 (Fig. 7f) have markedly a wave-number 1 pattern. Wind speeds are high at the southeastern side in SM1 and TY1. The area of high wind speeds is clearly found behind the typhoon. Although the asymmetric pattern of wind distribution is different among the three experiments, the values of simulated central pressure range 961 – 963 hPa at 60 h and their difference is small.

Figure 8 illustrates the horizontal distribution of significant wave heights in SM1 (Figs. 8a and 8d), JA1 (Figs. 8b and 8e) and TY1 (Figs. 8c and 8f) at 24 h (Figs. 8a-c) and 60 h (Figs. 8d-f) for Fanapi. At both 24 h and 60 h, significant wave heights are high on the right side along the track. The significant wave height at both 24 h and 60 h in TY1 is highest of all the experiments. The significant wave height becomes high to some extent ahead of Fanapi at 60 h in SM1. However, the significant wave height at 60 h tends to be high on the right side along the track in all the experiments.

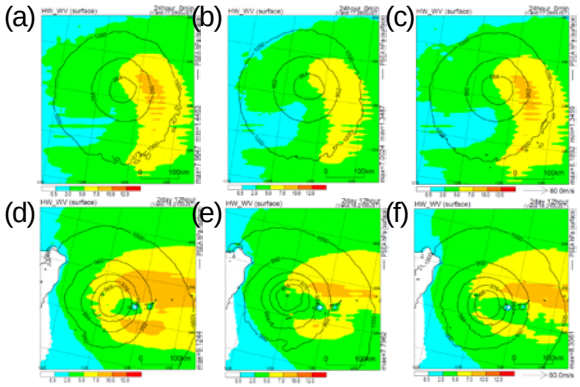

Figure 8 Same as Fig. 6 except for Fanapi.

The distributions of wind speeds at 20-m height for Choi-wan (Fig. 5) and Fanapi (Fig. 7) are related to those of surface roughness length for Choi-wan (Fig. 9) and Fanapi (Fig. 10). The values of surface roughness length except that in TY1 are high where wind speeds at 20-m height are high because surface roughness lengths in SM1 and JA1 are a function of frictional velocity (Table 1). The value of surface roughness length in TY1 is high at the southeastern side at 24 h (Fig. 9c) and 72 h (Fig. 9f), where significant wave height is high (Figs. 6c and 6f). In contrast, the value of surface roughness length in TY1 is low at the northeastern side at 24 h (Fig. 9c) and at the southwestern-southern side at 72 h (Fig. 9f) for Choiwan and at the southern part at 24 h (Fig. 10c) and 60 h (Fig. 10f) for Fanapi. These results indicate that surface roughness lengths level off at these areas. The value of surface roughness length is relatively small in JA1 for both Choi-wan and Fanapi, which is also seen in CH1 and KO1 (not shown). The value of surface roughness length has a peak ahead of the typhoon in SM1 and TY1, where 20-m wind speeds are relatively weak. This suggests that surface roughness lengths hardly level off ahead of the typhoon in the case of Fanapi.

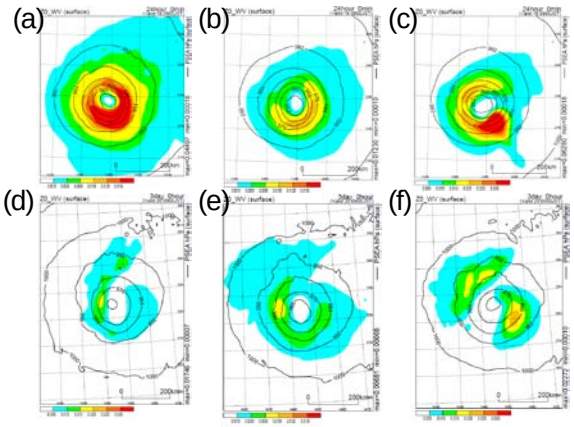

Figure 9 Horizontal distributions of surface roughness length at 24 h for Choi-wan in (a) SM1, (b) JA1 and (c) TY1 and 60 h in (d) SM1, (e) JA1 and (f) TY1.

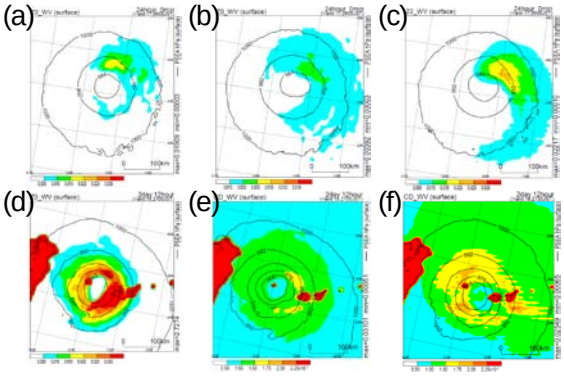

Figure 10 Horizontal distributions of surface roughness length at 24 h for Fanapi in (a) SM1, (b) JA1 and (c) TY1 and at 60 h in (d) SM1, (e) JA1 and (f) TY1.

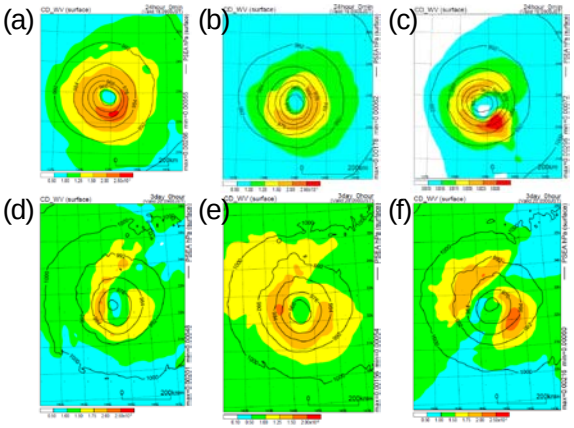

Figure 11 Same as Fig. 9 except for drag coefficient.

The horizontal distribution of drag coefficient in SM1, JA1 and TY1 is coincident with those of surface roughness lengths for both Choi-wan (Fig. 11) and Fanapi (Fig. 12). Once the horizontal distribution of surface roughness length is determined, that of drag coefficient is regulated by surface roughness length. The horizontal distribution of wind speeds at 20-m height is determined from that of surface roughness lengths and resultant drag coefficients except that in TY1. In TY1, however, drag coefficients level off where surface winds are high. The location differs depending on a phase of typhoon although it seems to appear on the left side behind a typhoon.

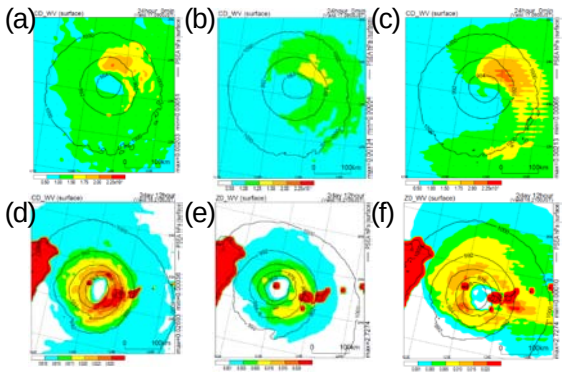

Figure 12 Same as Fig. 10 except for drag coefficient.

4. Discussion and conclusions

According to Kohno et al. (2006), drag coefficients tend to be scattered, but generally become high when wind speeds become high. From numerical simulations of Choiwan and Fanapi in this study, only drag coefficients calculated by the formulation based on wave steepness (Taylor and Yelland, 2001) level off when 10-m wind speeds are high. The value of high wind speeds differ depending on the case of typhoon and its developing phase. Thus, the result of this study does not deny that of Kohno et al (2006). The value of wind speed at the peak of surface roughness length and drag coefficient differs between Choi-wan and Fanapi and it depends on the phase (integration time) of these typhoons.

The results of sensitivity experiments suggests that longer surface roughness length and higher value of drag coefficient lead to weaker simulated typhoon and an asymmetric pattern of 20-m wind speed in the case of Choi-wan although there is little impact of surface roughness lengths on simulated tracks. The results have been already reported by Kohno et al (2006). A change in surface roughness lengths first affects surface wind speeds and then affects ocean waves and structural change in a typhoon. However, simulated central pressure in SM1 is lowest at 48 h in the case of Fanapi although values of surface roughness length and drag coefficient are relatively high among the three experiments. Why can simulated Fanapi intensify in SM1?

Higher drag coefficients are considered to strengthen the inflow near the surface, in the lowermost part of the atmospheric boundary layer. This may lead to the enhancement of secondary circulation within the inner core of Fanapi around 48 h. The reduction of tangential wind speeds due to surface friction has an essential effect on reducing the intensity in the case of Choi-wan. However, surface friction may lead to the intensification of Fanapi through the enhancement of secondary circulation.

How changes in surface roughness length and drag coefficient affect the intensity and structural change of Choi-wan and Fanapi is an individual and interesting issue and one of subjects we should address in future.

Acknowledgements:

This work was supported by the Japan Society for the Promotion of Science (JSPS), Grant-in-Aid for Scientific Research (C) (22540454) and on Innovative Areas (Research in a proposed research area) (23106505).

References

Charnock, H. (1955), Wind stress on a water surface, *Quart. J. Roy. Meteor. Soc.*, **81**, 639-640.

Jansen, P. A. E. M. (1991), Quasi-linear theory of wind-wave generation applied to wave forecasting, *J. Phys. Oceanogr.*, **21**, 1631-1642.

Edson, J., T. Crawford, J. Crescenti, T. Farrar, N. Frew, G, Gerbi and Coauthors (2007), The Coupled Boundary Layers and Air–Sea Transfer Experiment in Low Winds. *Bull. Amer. Meteor. Soc*., **88**, 341–356.

Kohno, N., A. Murata, and W. Mashiko (2006), The impact of roughness changes by sea state under typhoon field. *The 9th International Workshop on Wave Hinding and Forecast.* Victria, B.C., Canada, 24-29 Sept.

Kondo, J. (1975), Air-sea bulk transfer coefficients in diabatic conditions. *Bound. Layer Meteor.*, **9**, 91-112.

Louis, J. F., M. Tiedtke, and J. F. Geleyn (1982), A short history of the operational PBL parameterization at ECMWF. Proc. *Workshop on Planetary Boundary Layer Parameterization*, Reading, United Kingdom, ECMWF, 59–79.

Smith, S. D., R. J. Anderson, W. A. Oost, C. Kraan, N. Maat, J. Decosmo, K. B. Katsaros, K. L. Davidson, K. Bumke, L. Hasse, and H. M. Chadwick (1992), The HEXOS results. *Boundary-Layer Meteorol*., **60**, 109-142.

Taylor, P. K., and M. J. Yelland (2001), The dependence of sea surface roughness on the height and steepness of the waves. *J. Phys. Oceanogr.*, **31**, 572-590.

Usui, N., Ishizaki S., Fujii Y., Tsujino H., Yasuda T., and Kamachi M. (2006), Meteorological Research Institute multivariate ocean variational estimation (MOVE) system: Some early results. *Advances in Space Research*, **37**, 896-822.

Wada, A. (2009), Idealized numerical experiments associated with the intensity and rapid intensification of stationary tropical cyclone-like vortex and its relation to initial sea-surface temperature and vortex-induced sea-surface cooling, *J. Geophys. Res*., **114**, D18111.

Wada, A., N. Kohno and Y. Kawai (2010), Impact of wave-ocean interaction on Typhoon Hai-Tang in 2005, *SOLA*, 6A, 13-16.